

# FLAR, ODAR, ship's radar

by Ture Hagman, Jerry Nilsson  
and Yngve Nilsson  
Stockholm 1976

*Cover picture:  
The icebreaker TOR in the middle  
of the test area for SEA ICE —75  
and an example of an ODAR re-  
gistration over the Bay of Bothnia.*

# SEA ICE 75

## FLAR, ODAR, ship's radar

Ture Hagman

Jerry Nilsson

Research Institute of National Defence, Sweden

Yngve Nilsson

Swedish Administration of Shipping and Navigation

Stockholm 1976



Printed in Sweden  
DIREKTOFFSET  
Norrköping 1976

# Table of Contents

<b>Foreword</b> .....	4
<b>Summary</b> .....	5
<b>1. Introduction</b> .....	6
1.1 Flight Program .....	6
<b>2. Experimental Results</b> .....	7
2.1 ODAR Measurements .....	7
2.2 FLAR Measurements .....	11
2.3 Comparison of FLAR, SLAR and High Altitude Photos .....	13
<b>3. Ship's Radar</b> .....	15
3.1 Introduction .....	15
3.2 Summary of Obtained Results .....	15
3.3 Material Used for Analysis .....	15
<b>4. Discussion</b> .....	29
4.1 Radar Signatures of Different Types of Ice .....	29
4.2 Range Limitations .....	29
4.3 Mapping Capacity of Airborne Radars .....	29
4.4 Weather Dependence .....	30
<b>5. Conclusions and Recommendations</b> .....	31
<b>References</b> .....	32

# Foreword

The Winter Navigation Research Board presents report No. 16:5. During the remote sensing experiment SEA ICE-75 a number of active microwave instruments were tested with respect to their ability to map various sea ice features. This report presents the results from the tests of three sensors of the same nature, namely the Forward Looking Airborne Radar (FLAR), the Omnidirectional Airborne Radar (ODAR) and the Ships Radar. The National Defence Research Institute was responsible for the FLAR and the ODAR in cooperation with the Swedish Airforce and the Swedish Navy. The captain on the icebreaker TOR was responsible for the operation of the Ships Radar.

The Winter Navigation Research Board wish to warmly thank the authors of this report as well as all other individuals, Institutions and Organizations, who contributed to the experiemnt SEA IC-75 in such a remarkable cooperative spirit.

Norrköping and Helsinki; July 1976.

**Lennart Johansson**

**Helge Jääsalo**

## Summary

This report describes results from a field test on sea ice mapping by radar. The experiment was carried out in the Gulf of Bothnia, March 1975.

Three different types of radar were used: forward looking airborne search radar (FLAR), omnidirectional helicopterborne search radar (ODAR) and shipborne radars of the icebreaker Tor.

It is shown that conventional radars can map the large scale ice structure of extensive areas in sufficient detail to assist navigation and iceforecasting. The radars of an icebreaker give short range navigational information on the ice situation with high resolution in real time.

Trained radar operators should be able to extract information on type of ice, location of big leads and areas of heavily ridged ice.

Different ways of recording radar information are discussed and some recommendations on further measurements of radar signatures of sea ice are given.

# 1. Introduction

During march 1975 a field experiment for remote sensing of sea ice was performed in the Gulf of Bothnia. Details on the program in (1).

In order to study the possibilities to map the sea ice irrespective of weather conditions and time of day different radar systems were tested during the experiment. This report deals with data obtained from conventional airborne search radars, one forward looking radar (FLAR) mounted in a Pembroke aircraft and one helicopterborne radar with a 360° azimuthal scan (ODAR). The report also includes a section of PPI photos from the 10 cm and 3 cm radars on board the icebreaker Tor. The shipborne radars give short range navigational information on the ice situation with high resolution. Measurements using sidelooking radar (SLAR) are treated separately in (2).

	FLAR	ODAR	TOR	
Frequency	X-band	X-band	X-band	S-band
Peak pulse power	70 kW		45 kW	60 kW
Resolution:				
range	45 m and 150 m	50 m and 120 m	9 m and 90 m	12 m and 90 m
azimuth	3.5°	3°	0.7°	1.8°
Antenna polarization	Horizontal and vertical	Horizontal	Horizontal	Vertical
Search program	±60° in azimuth. Manually controlled antenna elevation.	360° in azimuth. Manually controlled antenna elevation.	360° in azimuth	
Indicators	Two 5-inch PPIs	12-inch PPI; North stabilized	16-inch PPI; North stabilized	

Table 1. Technical data of the radar equipment.

The PPI-information of the radars was recorded as follows.

**FLAR:** 16 mm film recording with one antenna scan on each frame using a motordriven camera controlled by the antenna program unit.

During some of the flights radar video and antenna position were stored on magnetic tape using a standard TV video tape recorder.

**ODAR and TOR:** 35 mm manual camera using black and white film.

The photographic documentation of the radar information has some limitations which must be kept in mind when studying the experimental results. Standard radar indicators are optimized not to mapping but to detection of small targets in clutter environment. This means in practise that the cathode ray tubes of the indicators are adapted to the eye of a human operator providing him with a picture with a limited number of grey levels. The intensity of the targets is a function of the phosphorescence of the tube, which is not linearly proportional to the tube, which is not linearly proportional to the video signal. The rapid fluorescence normally used for photographic reproduction, for instance in flying spot scanners, is as a rule attenuated by optical filters. The exposure of the film will always be a compromise as the light intensity per unit area is different at the center and edge of the indicator due to the radial scan. The results is an over exposure of the central parts and an under exposure of the peripheral parts of the PPI. The number of grey levels of the indicator is further reduced when the photographic film is reproduced as a positive paper copy as this process too is nonlinear. This explains the black and white appearance of the PPI photos. A further reduction of the information is due to the fact that a photo gives a frozen situation without the dynamics of the actual situation available to the radar operator.

## 1.1 Flight program

During the experiment 8 flights were made with the FLAR equipment. Altitudes and covered areas are listed in table 2.

Table 2. FLAR flights during Sea Ice 1975.

Date	Altitude	Covered areas
11/3	450 m	Swedish 15x15 km area Preliminary tests
12/3	100 m 450 m	Swedish 15x15 km area Preliminary tests
13/3	100 m 250 m 450 m	Swedish 15x15 km area
14/3	50 m 450 m	Same as the SLAR 14/3
17/3	100 m 250 m	Swedish 15x15 km area Preliminary tests
18/3	100 m 450 m	Same as the SLAR 18/3
19/3	100 m 450 m	Finnish and Swedish 15x15 km areas
21/3	1800 m	Malören-Bjuröklubb Holmön

Table 3. ODAR flights during Sea Ice 1975.

Date	Altitude	Covered areas
18/3	100 m 200 m 300 m 500 m	Swedish 15x15 km area
19/3	30 m 170 m 300 m 700 m	Swedish 5x5 km and 15x15 km areas
19/3	30 m 170 m 1000 m 1000 m	Swedish 5x5 km and 15x15 km areas. The northern parts of the Bay of Bothnia.
20/3	700 m	The northern parts of the Bay of Bothnia

## 2. Experimental Results

The azimuthal resolution and PPI scales of the two airborne radars are such, that the equipment is mainly suitable for medium and large scale mapping of the gross structure of the ice. As the main part of the ground truth program was concentrated in the vicinity of the icebreaker Tor, within the 5x5 km area, there exist only a few high altitude photos (March 13th and 17th) and one satellite photo that can be compared to the radar data. From the long triangular flights of march 14th and 18th the only ground truth available is the notes made by the aircrew during the flights.

### 2.1 ODAR measurements

As the helicopterborne radar was available for a very limited time, no test flights could be made before the experiment. The flights of March 18 and 19 were preliminary tests to find out how the system could be used for ice mapping. The radar is not primarily intended for navigational purposes and it showed up that the receiver used in connection with the 0.35  $\mu$ s pulse could not be used for mapping. This fact limited the possibilities of obtaining short range pictures with high resolution and the PPI-photos dealt with in this report are all made with medium or long range scale using 0.8  $\mu$ s pulse length. The PPI is north stabilized on all photos. Shadow sectors due to the rear wheels of the helicopter are visible approximately 45° left and right of the radial heading marker.

March 18th a test was made to find out the visibility of the radar reflectors of the 5x5 km area at different flight levels. Fig 1 to 4 is a series of PPI-photos at altitudes 300, 600, 900 and 1500 feet. The gain of the radar receiver and the light intensity of the indicator have been kept at the same level during the climb. At the actual gain setting which is chosen to show the reflectors with high contrast when the helicopter is hovering at 300', the ice structure is mapped out to a distance where the grazing angle is approximately 1.5°. Outside this area some ice-echoes from high ridges are visible. The grazing angle dependence of the backscatter from the ice surface is also demonstrated in these photos. If we regard the mapping capacity of the radar at a fixed distance for instance 12 km, which is the distance to Tor, we find at flight level 300 echoes from Tor, the reflectors, marked by arrows, and some ice structure probably ridges

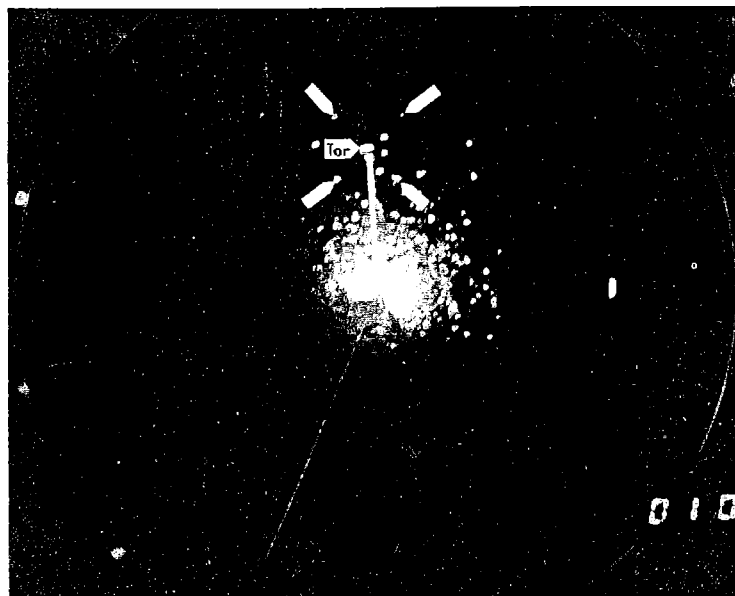


Figure 1. PPI ODAR 750318, altitude 300'.

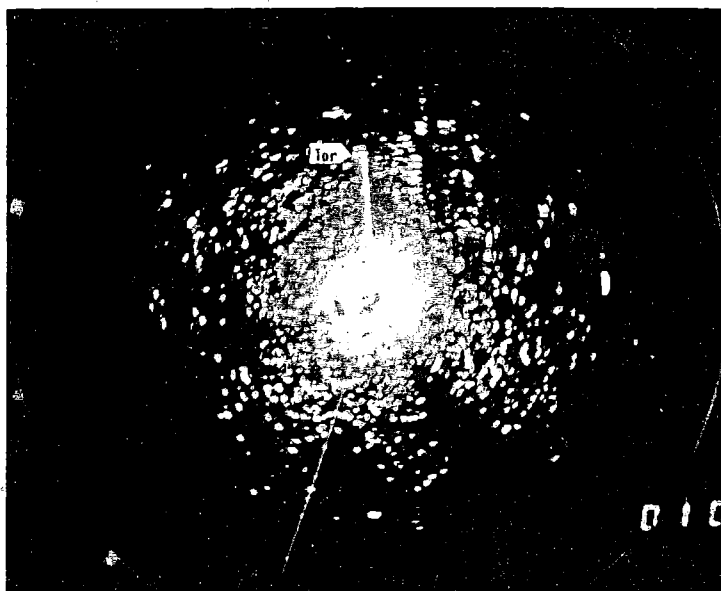
0 10 20 km

Figure 2. PPI ODAR 750318, altitude 600'.



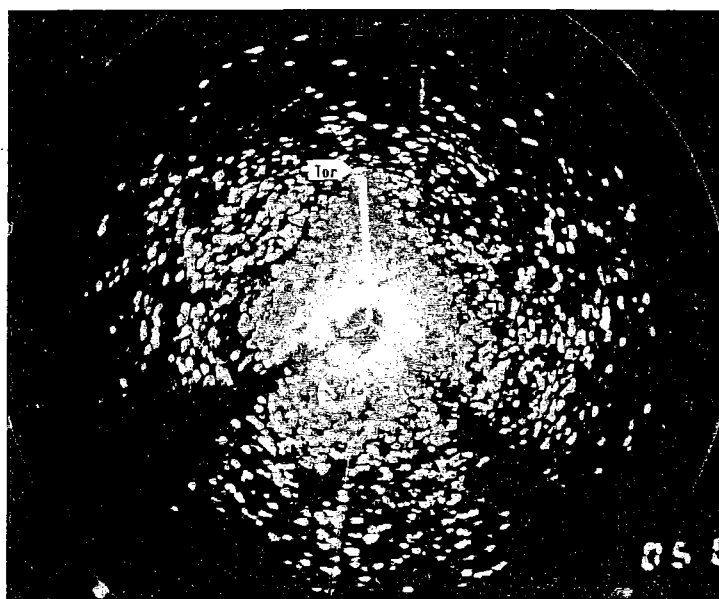
0 10 20 km

Figure 3. PPI ODAR 750318, altitude 900'.



0 10 20 km

Figure 4. PPI ODAR 750318, altitude 1500'.



0 10 20 km

2 km east of Tor. Grazing angle at the distance to Tor is  $0.4^\circ$ . At altitudes 600' and 900', grazing angle  $0.9^\circ$  and  $1.3^\circ$  respectively, the number of ice-echoes increase and the large scale structure of the ice begins to show up. Note for instance the bowformed lead 5 km southeast of Tor. Flight altitude 1500' gives a further increase of the density of ice-echoes and areas of high ridge density may be distinguished from level ice and open water areas. The radar reflectors of the 5x5 km area not distinguishable from the ice echoes at grazing angles larger than approximately  $1.5^\circ$ .

At 1500' the mapping range of the ODAR is approximately 65 km and overlay maps of very large areas are obtainable. Fig 5 shows a radar map of the total ice extension in the northern parts of the Gulf of Bothnia on the 20th of March 1975. The radar map is made from two PPI-photos from the ODAR. Heavily ridged areas east of Malören, a lead south of this area and a system of leads west and southwest of Karlö are clearly visible as well as open water in the western part of the Gulf of Bothnia. Black areas north of Malören and along the Finnish coast are level land-fast ice with low reflectivity. The radar map may be compared to the high altitude satellite photo in fig. 6. This photo is of the type normally used in ice forecasting and it is obvious that the radar map gives more details on the ice situation. The radar has also got the advantage of been relatively insensitive to meteorological conditions, whereas satellite photos are obtainable only during daytime and fine weather.

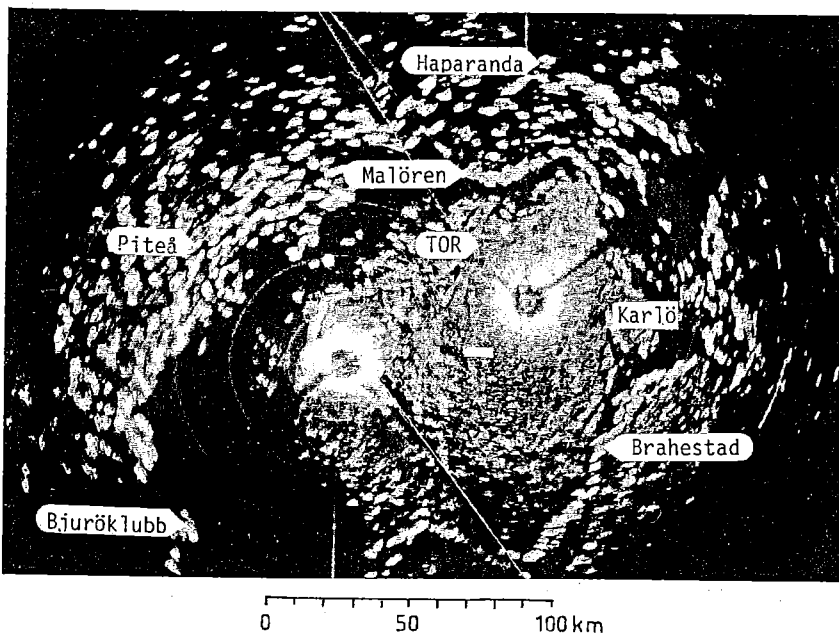


Figure 5. ODAR 750320. Ice extension in the northern part of the Gulf of Bothnia.

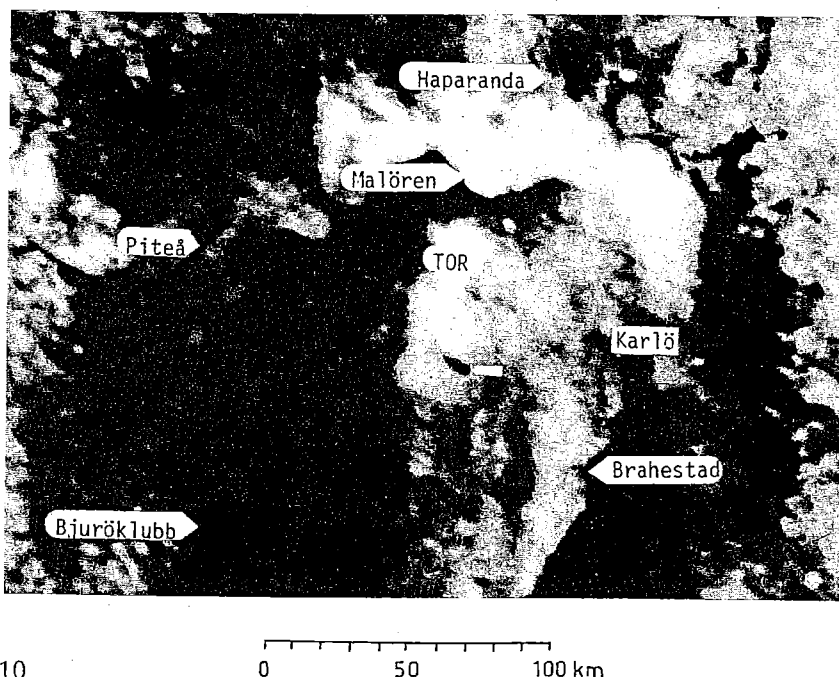


Figure 6. Weather satellite picture of the same area as in fig 5.

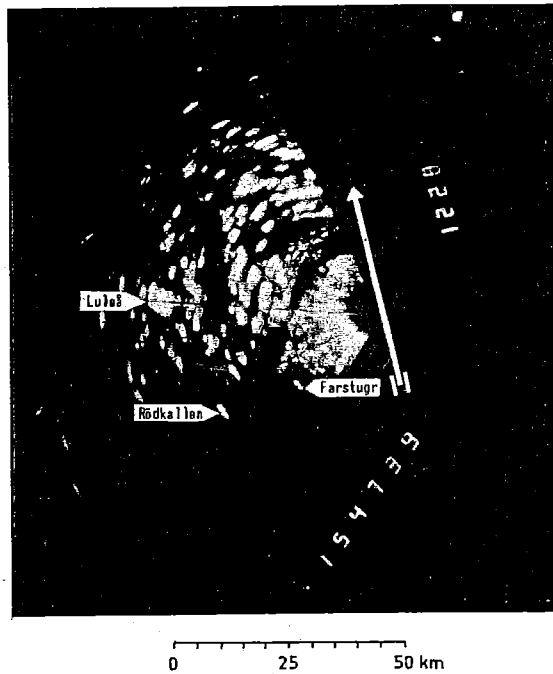
## 2.2 FLAR measurements

During the experiment the mapping capacity of the FLAR was tested at flight levels between 100' and 6000'. No definite differences in mapping quality was observed at different flight levels. The coverage of the radar was however limited by the dynamic range of the receiver at flight levels below 750', as the relative strength of near zone echoes and echoes at the edge of the indicator (range scale 20 km) was very different and could not be compensated for by the range swept gain of the radar. This is however a problem that would not affect a radar designed for mapping.

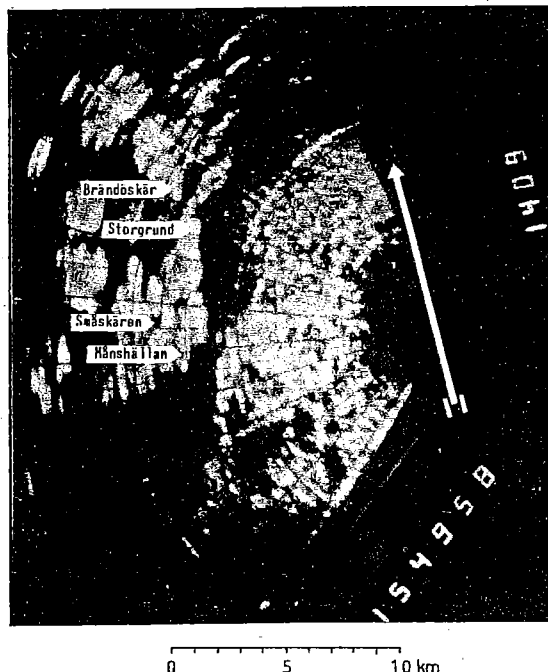
Fig 7 and fig 8 exemplify the method of positioning the FLAR photos using range scale 80 km to obtain an overlay view of the situation and range scale 20 km to study the ice situation in detail. The overlay photos are reproduced to the scale 1:1000 000 and the short range photos to 1:200 000.

Fig 7 shows the archipelago and ice situation east of Luleå march 11th. East of a line Småskären-Brändöskär is a narrow lead shown in detail in fig 8. Shallow waters west of the lead are covered with high iceridges visible as a bright line with high reflectivity outside and between Småskären and Brändöskär. Further west the ice between the islands is flat and snow-covered with low reflectivity, black in the photo. The lead is not covered with new ice which can be found from the flickering seascatter present on the PPI-film.

**Figure 7.** FLAR 750311, altitude 1500'; Overlay picture of archipelago and ice situation east of Luleå.



**Figure 8.** FLAR 750311, altitude 1500'; Detail of lead east of a line Småskären — Brändöskär, radar range 20 km.



During two of the flights the antenna unit of the radar was changed to vertical polarization. The change gave no noticeable effect except for a possible slight reduction of the backscatter level, which, however, cannot be proved from available data and therefore should be further examined. Fig 9 and 10 are PPI photos of the iceedge southeast of Bjuröklubb march 14th. Polarization of the radar: vertical.

As single frames of photographic recording only gives a small part of the information available for the radar operator an edited version of the PPI-film of march 17th has been prepared. The film, with comments, is available on request at the Defence Research Institute. Replayed at 12 frames/sec the film gives a ten to one timecompression of the flight and shows the dynamics of the PPI information.

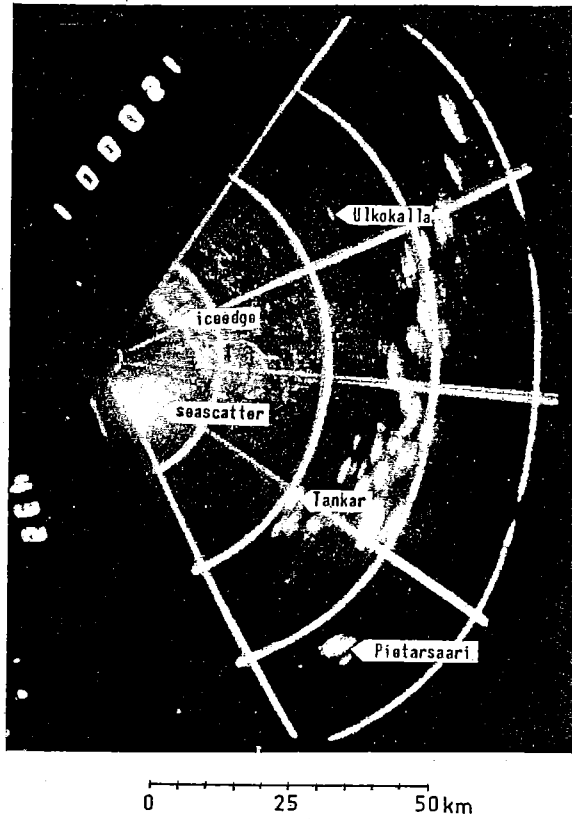


Figure 9. FLAR 750314, altitude 1500', vertical antenna polarization; Overlay picture of ice edge south-east of Bjuröklubb.

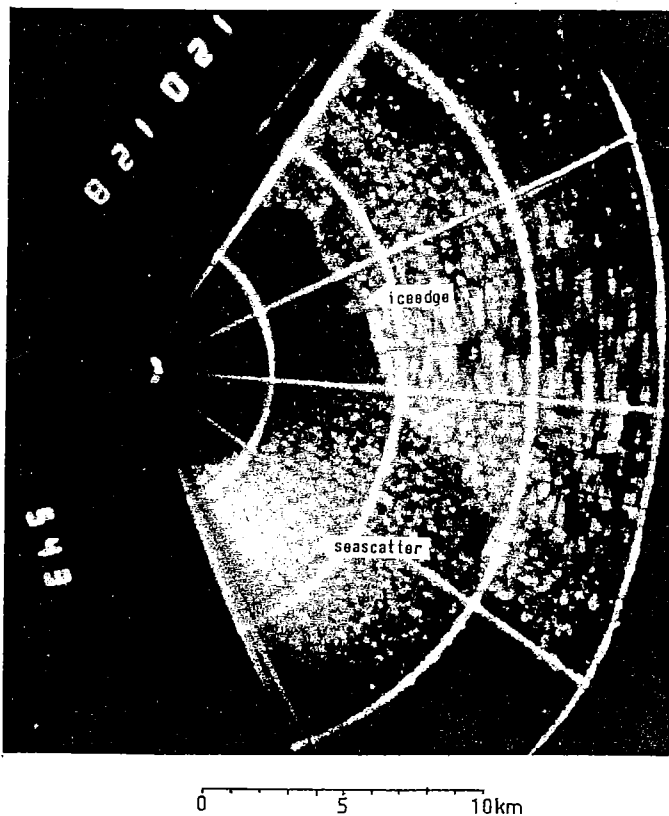


Figure 10. Detail of same ice edge as in fig 9, radar range 20 km.

### 2.3 Comparison of FLAR, SLAR and high altitude photos

Some of the FLAR registrations have been used for photo mosaics which can be compared to SLAR maps and high altitude photos. High altitude photos made by the Swedish airforce on march 17th and a FLAR mosaic of the area round and northwest of Tor are shown in fig 11. The main features of the ice, large floes and leads are marked with numbers. The time difference between the flights is 3.5 hours and during that time the ice situation shifts as the ice mass drifts southwards. The lead at 5, for instance, grows narrower which can be seen in the photographs made by the Land Survey at 15 o'clock the same day. The well defined black area 2 km west of the number 3 is probably a new lead formed during the day. The difference between the relatively flat ice round Tor and the ridged and cracked areas east of lead 5 may also be seen in the radar map.

**Figure 11.** Comparison of FLAR mosaic and high altitude photos of the area north-west of TOR, 750317.

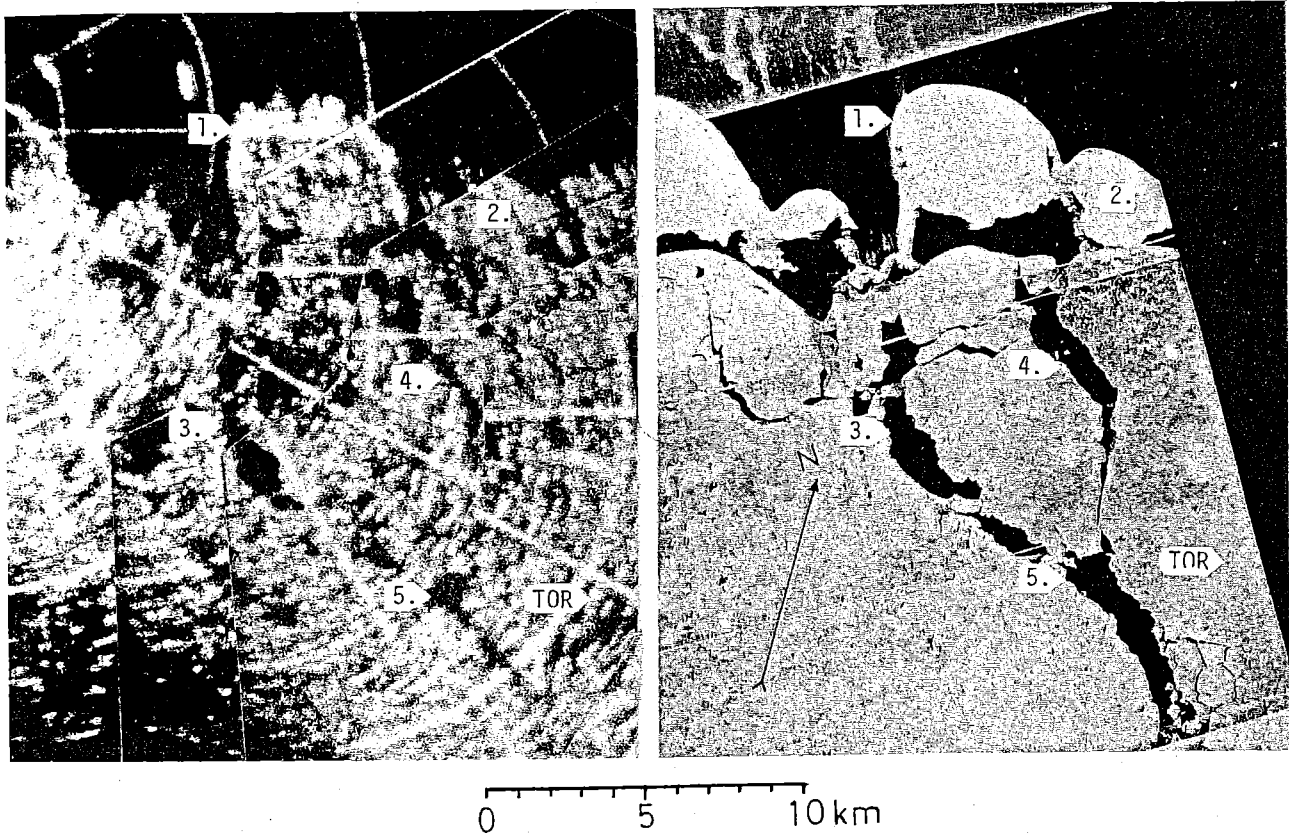
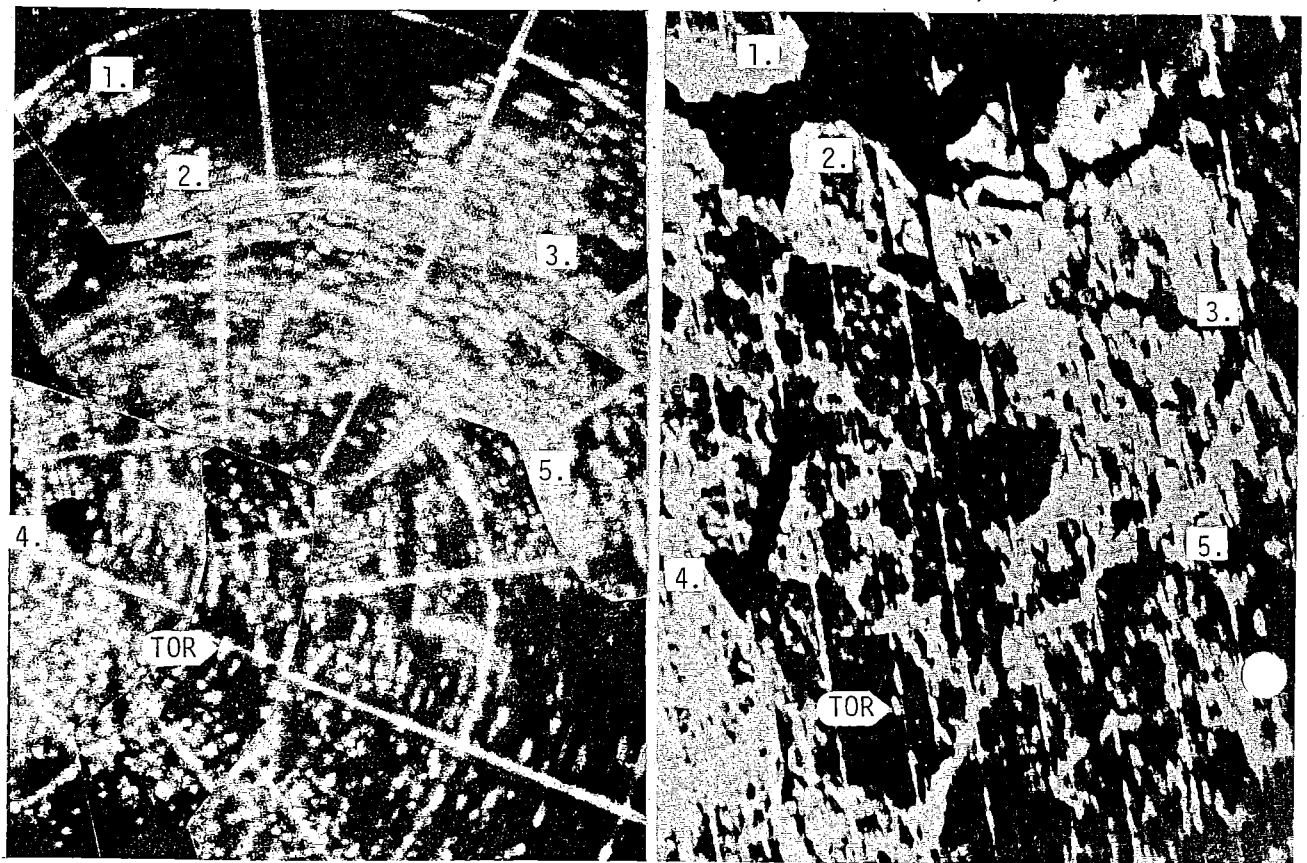


Fig 12 is a comparison of FLAR and SLAR mapping of the area round Tor on the 18th of march. The ice edge at the lead south of Malören is at the top of the maps, markings 1 and 2. 4 is a characteristic lead northwest of Tor developed during the night from the intersection of leads 4 and 5 of fig 11. Tor is shown in the middle of a flat ice area surrounded by cracked and ridged ice and leads to the west south and east. The structure of the relatively flat ice round Tor may be mapped by increasing the gain of the radar but this causes a saturation of the radar indicator at the areas with ice roughness.

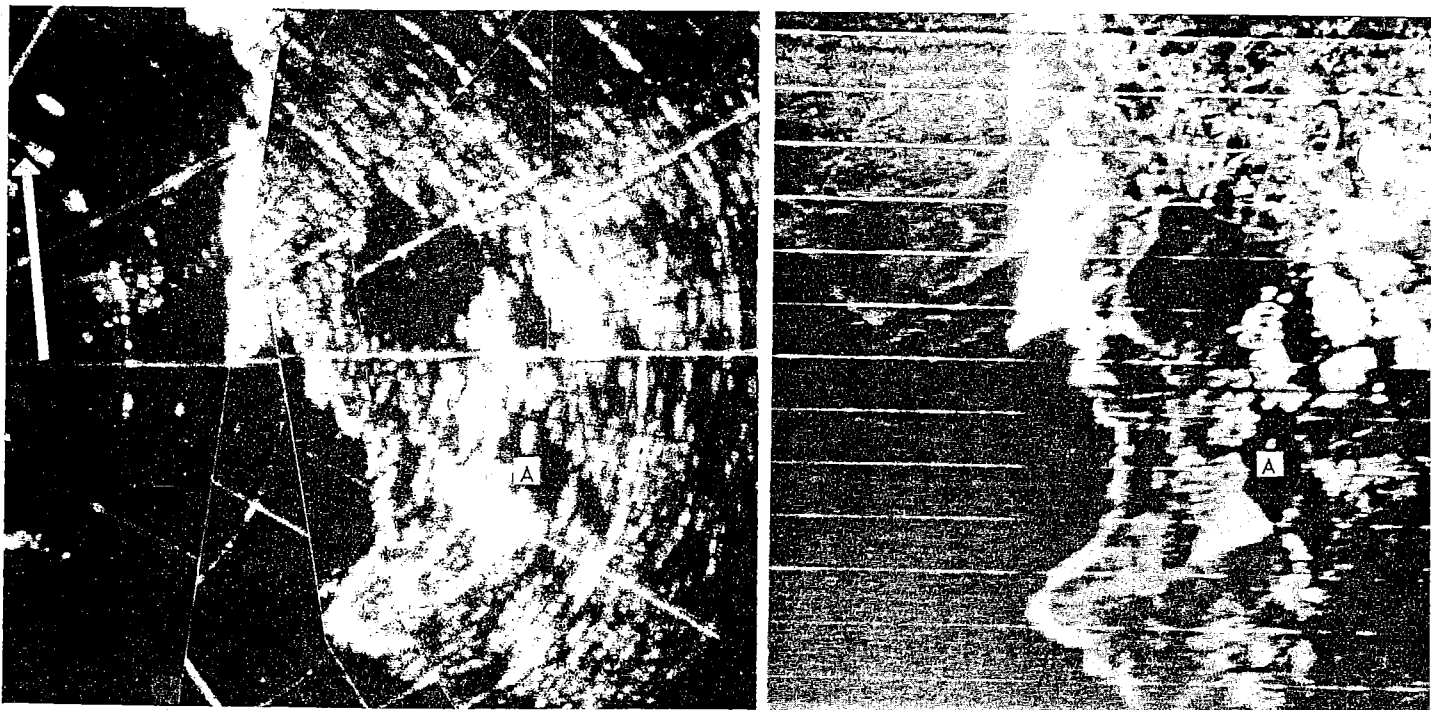
Fig 13 shows the ice edge 36 km of Bjuröklubb march 18th. Flight altitudes of SLAR and FLAR aircrafts are 20000 feet and 1500 feet. Left (west) of the ice edge is open water with strings of slush ice and some drifting floes. The ice edge consists of many small floes pressed together by the wind. East of the edge loosely packed bigger floes separated by areas with open water and new ice. The difference in azimuthal resolution between SLAR and FLAR is demonstrated in these photos. Note for instance the point echo at A in the SLAR photo which in the FLAR picture is broadened by approximately 3.5 times which equals the ratio between the antenna beamwidths of the two radars. The main features of the ice are, however, mapped in a similar fashion in spite of the large differences in integration times and grazing angles of the two systems. The apparent angular discrepancies between the maps are due to uncorrected drift of the SLAR aircraft.

Figure 12. FLAR mosaic and SLAR image of the area round and north of TOR, 750318.



0 5 10 km

Figure 13. FLAR mosaic and SLAR image of ice edge 36 km east of Bjuröklubb, 750318. Flight altitudes: FLAR — 1500', SLAR — 20000'.



0 5 10 km

## 3. Ship's Radars

### 3.1 Introduction

This chapter describes the results obtained at a field test on sea ice mapping by the ship's radars of the icebreaker Tor.

During the whole ice investigation only small changes of the ice situation took place in the area near Tor. This contributed to the fact that every day on the whole the ship's radars gave the same results.

The analysis of the radar photos doesn't pretend to be scientifically made. It is based on comparisons with "Ground Truth", high altitude photos and is also based on practical experience from ship's radar ice detection.

When analysing certain comparisons with other radar sensors ODAR and SLAR, have been made.

The ship's radar is used operatively by icebreakers and merchant ships to find the best way through the ice in the surroundings. This is necessary in darkness and when the visibility is bad.

### 3.2 Summary of obtained results

1. The heights of the antennas on the ship's radars, 22—24 m above water level, provided good information of the ice situation at a distance of 0—1.5 n m.

At a distance up to 2.7 n m the ship's radars provided on special occasions some indications of the ice situation.

Separate ridges,  $h > 2-3$  m, gave the radar echoes at a distance of up to 3.5 n m.

2. The (X-band)  $\lambda = 3$  cm radar, gave a clearer picture of the ice in the immediate surroundings of the Tor than the (S-band) radar  $\lambda = 10$  cm.

The 10 cm radar obtained ice-ridges at a longer distance than the 3 cm radar.

The condition of the ship's radar (trimming) and variations in tuning of the radar were of great importance to interpret the ice situation.

3. The ship's radar can see the difference between
  - open water — ice
  - open water — ice edge — pack ice floes
  - ice ridges — level ice
  - different types of ice, for example vast thick ice floes refrozen to the surrounding level ice.
4. The ship's radar gave a good idea of the wideness and the extension of the ice ridges.
5. The ship's radar cannot see the difference between
  - snow-covered ice — snow free ice  
unless the snow-covered ice is very rough
  - the height of the ice ridges
  - the thickness of the ice
  - a narrow channel or a crack — a small ridge.

### 3.3 Material used for analysis

The analysis of the radar-photos from icebreaker Tor is based on information from extracts of SMHI "Ground Truth" as regards ice level-rafting, the height of the ridges, the extension and the concentration of the ridges and on information from the high altitude photos.

Comparisons have also been made with photos from other radars such as ODAR and SLAR.

The PPI-photos from the radars of the icebreaker Tor are listed in Table 4.

Characteristic features of the ice area are shown in fig 14 to fig 25.

1975-03

**Table 4.** PPI-photos from the radars of the icebreaker TOR.

Radar	Date	11	12	15	16	17	19	Sum
X-band	Numbers	-	4	3	4	3	3	17
S-band	Numbers	3	6	3	4	4	3	23
Sum		3	+ 10	+ 6	+ 8	+ 7	+ 6	= 40

Figure 14. Icebreaker TOR in the investigation area.

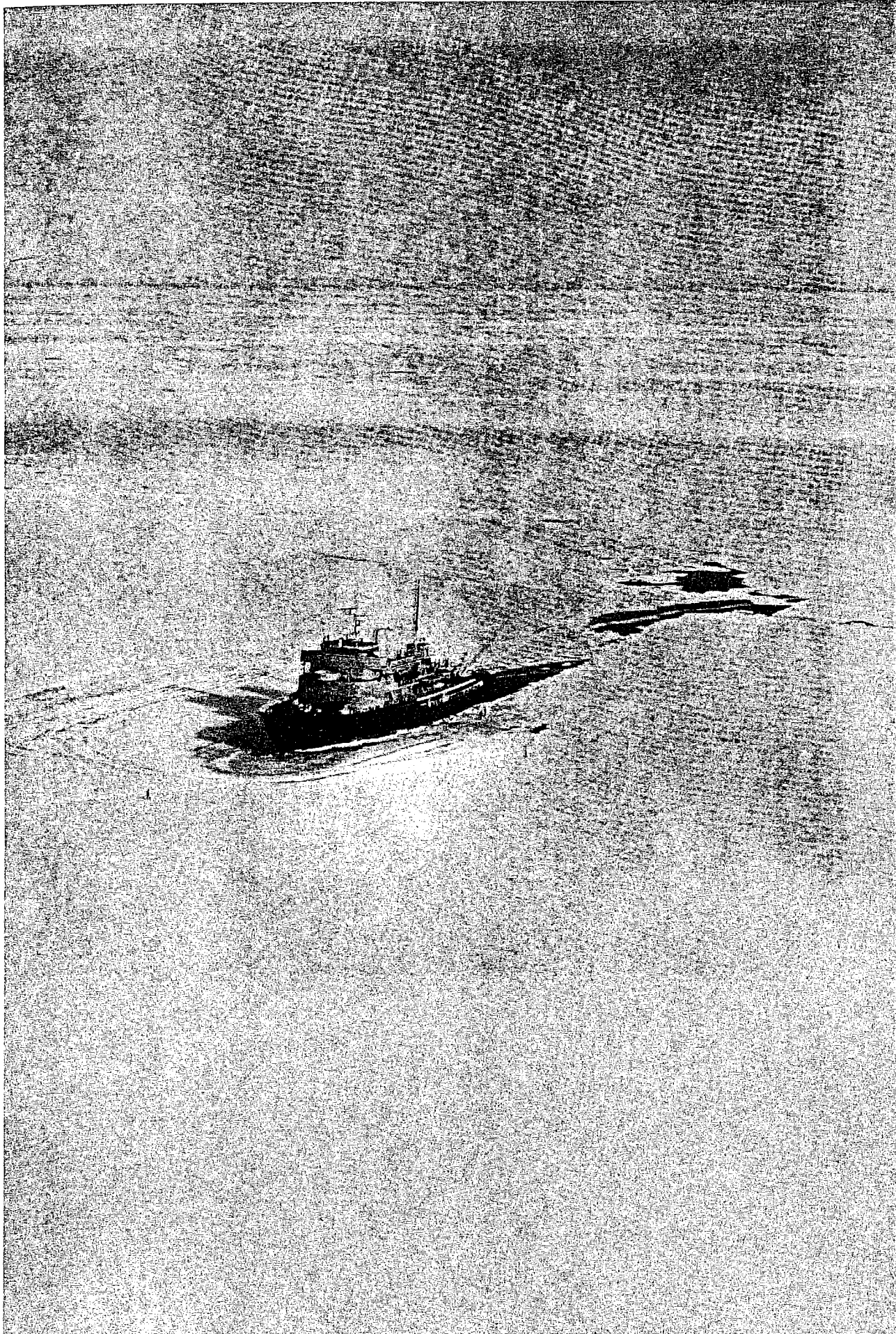


Figure 15—16. Comparison between photos X-band radar, range 1/2 n m — high altitude photo — "Ground Truth".

Figure 15.

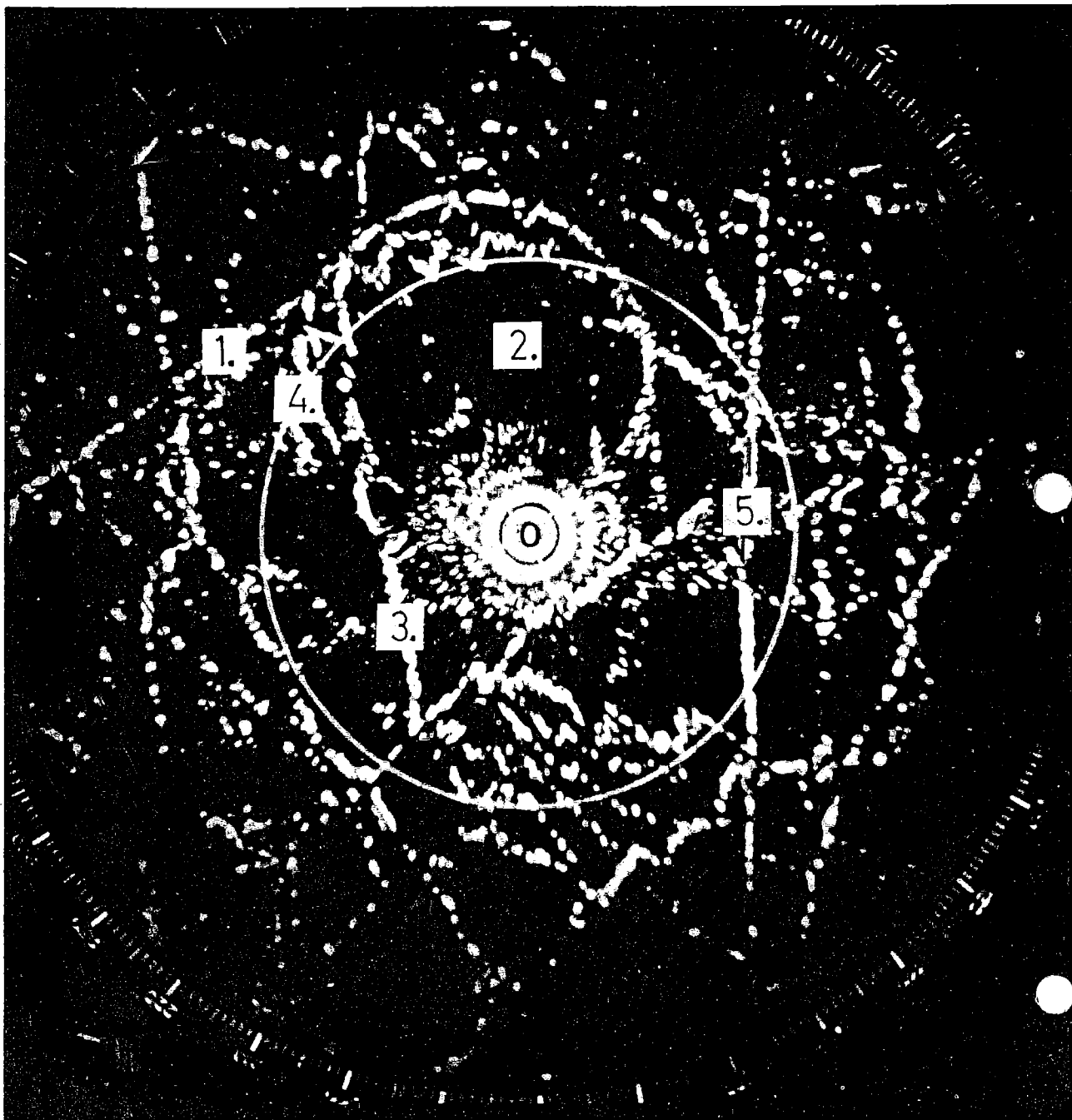


Figure 16.

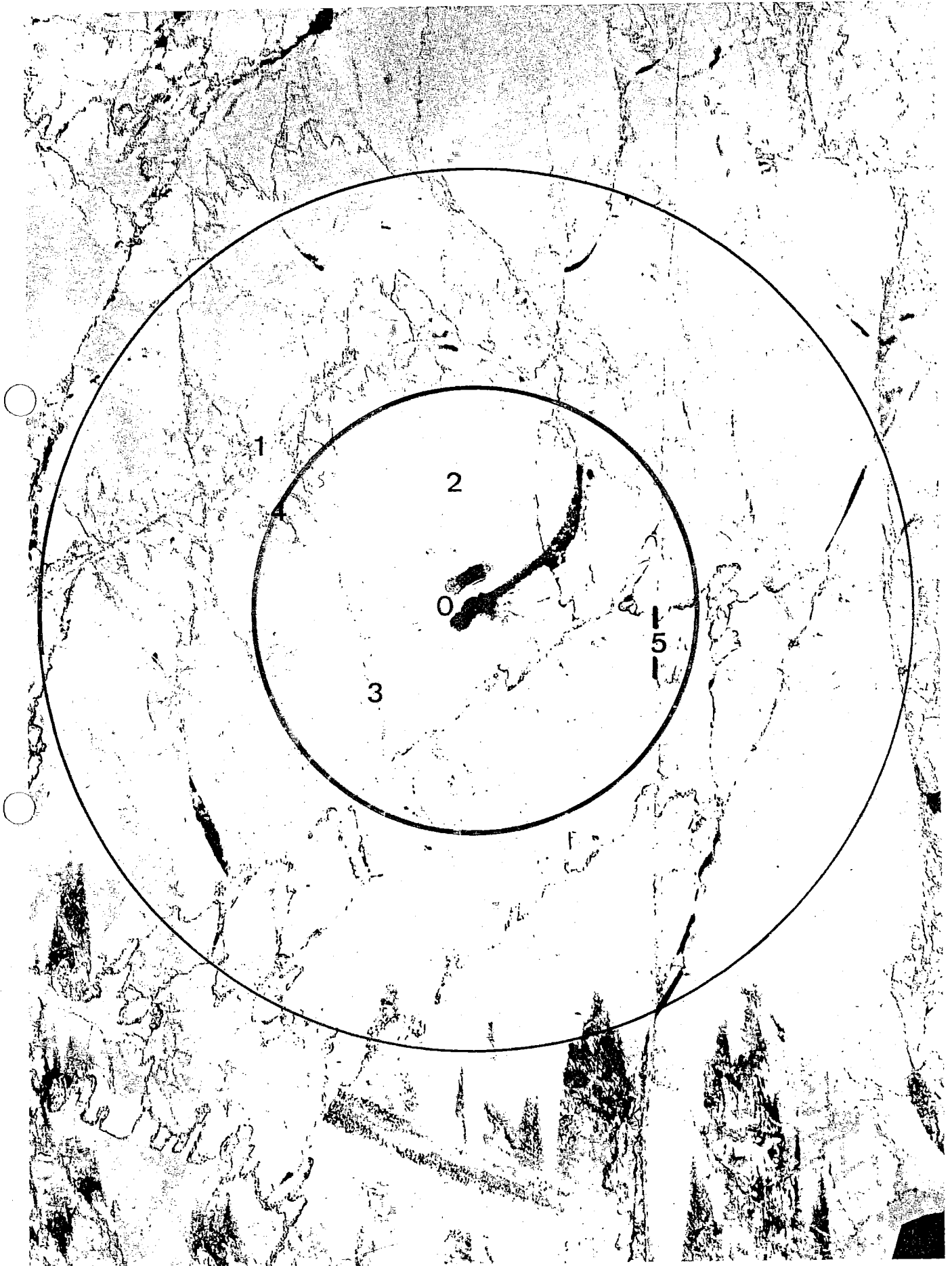


Figure 17—18. Comparison between photos X-band radar, range 3 n m — high altitude photo — "Ground Truth".

Figure 17.

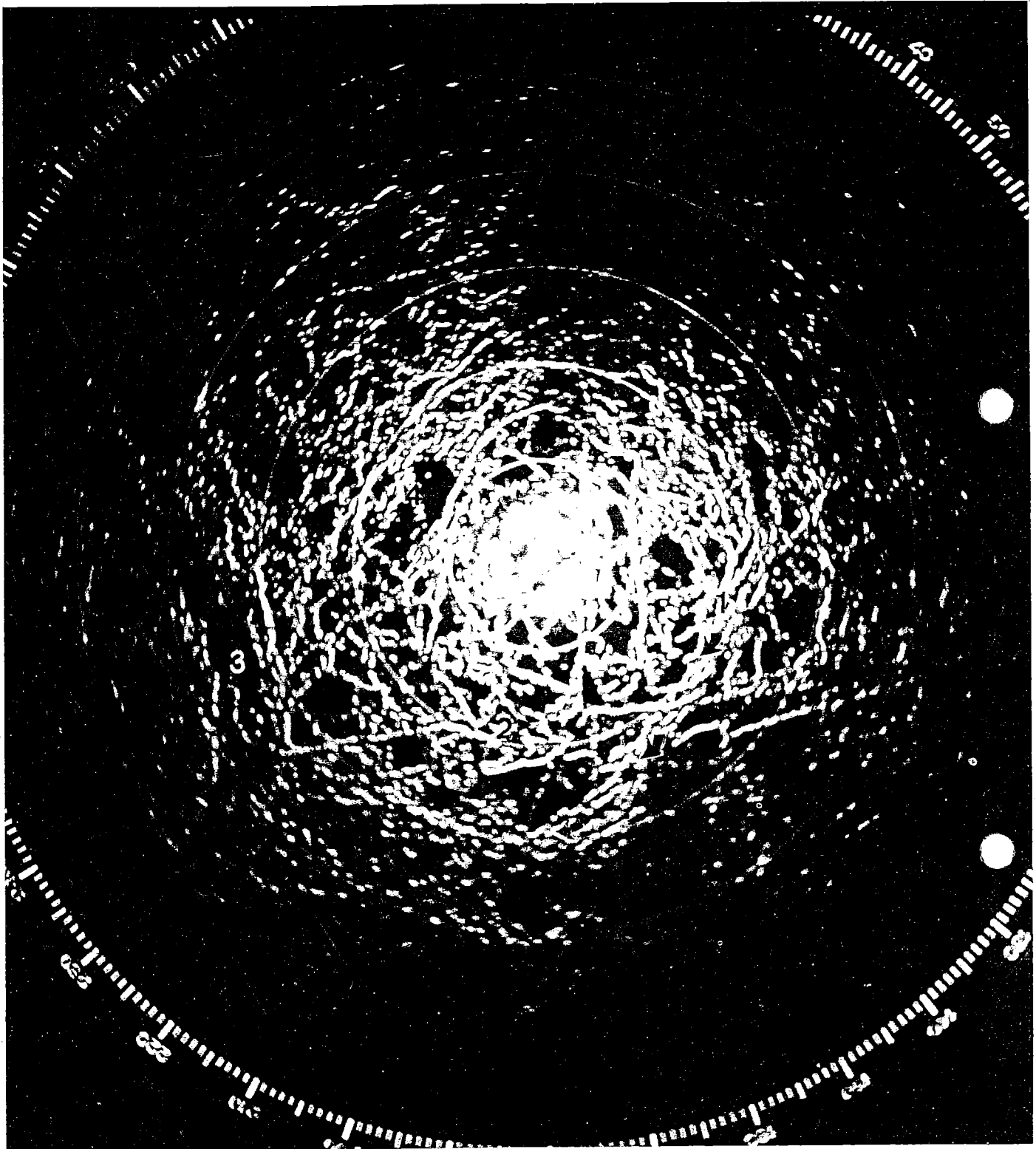


Figure 18.



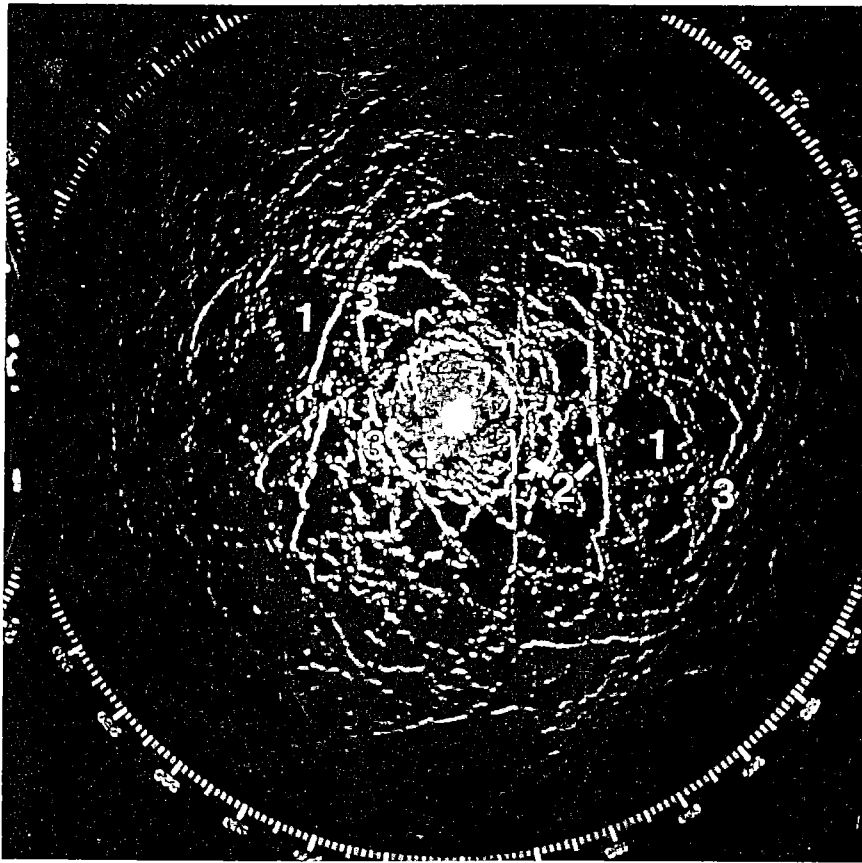


Figure 19—20. Comparison between X-band radar, range 1.5 n m — high altitude photo — "Ground Truth".

Figure 19.

Figure 20.



Figure 21—22. Comparison between X-band radar — S-band radar.

Figure 21.

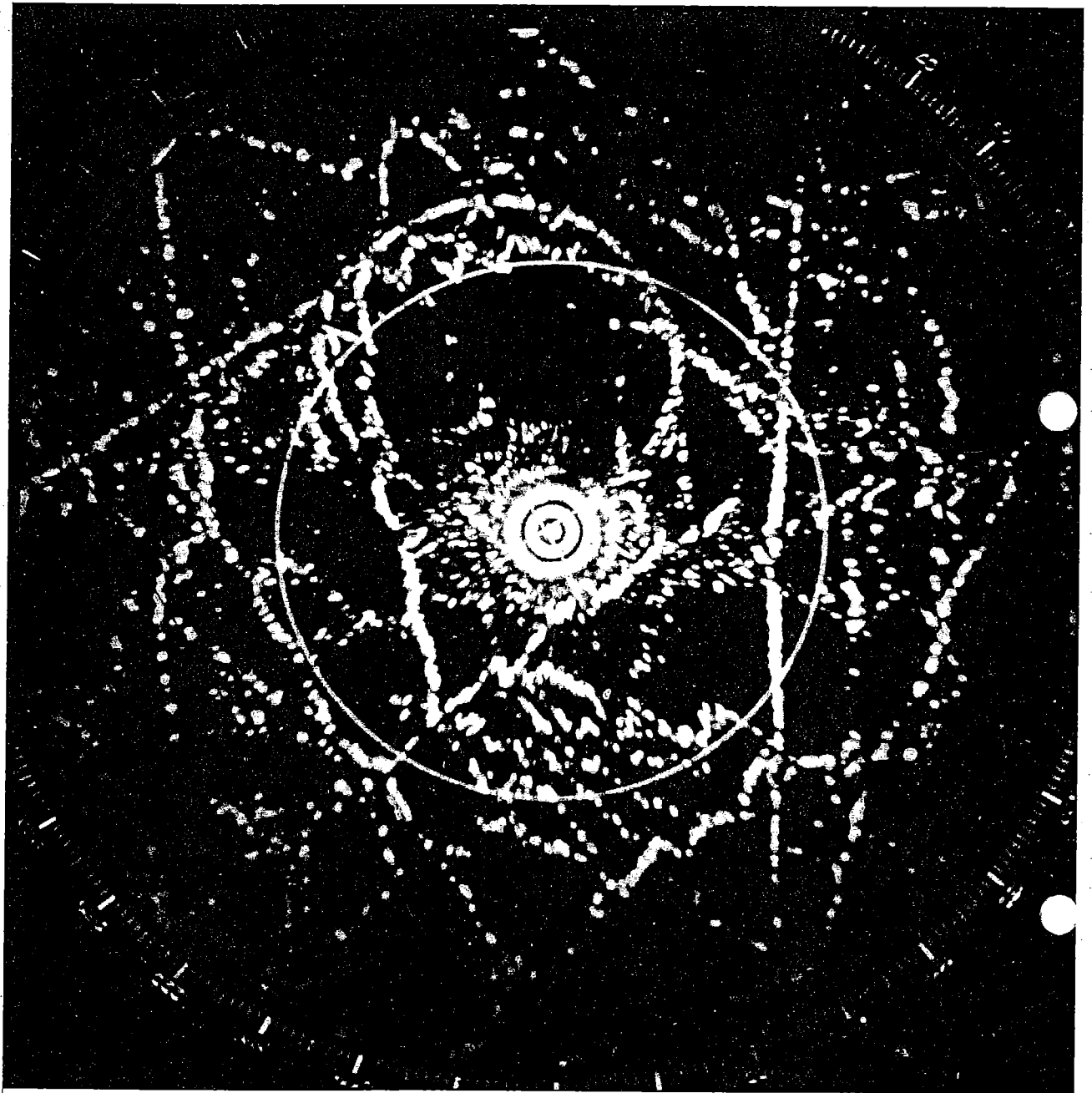


Figure 22.

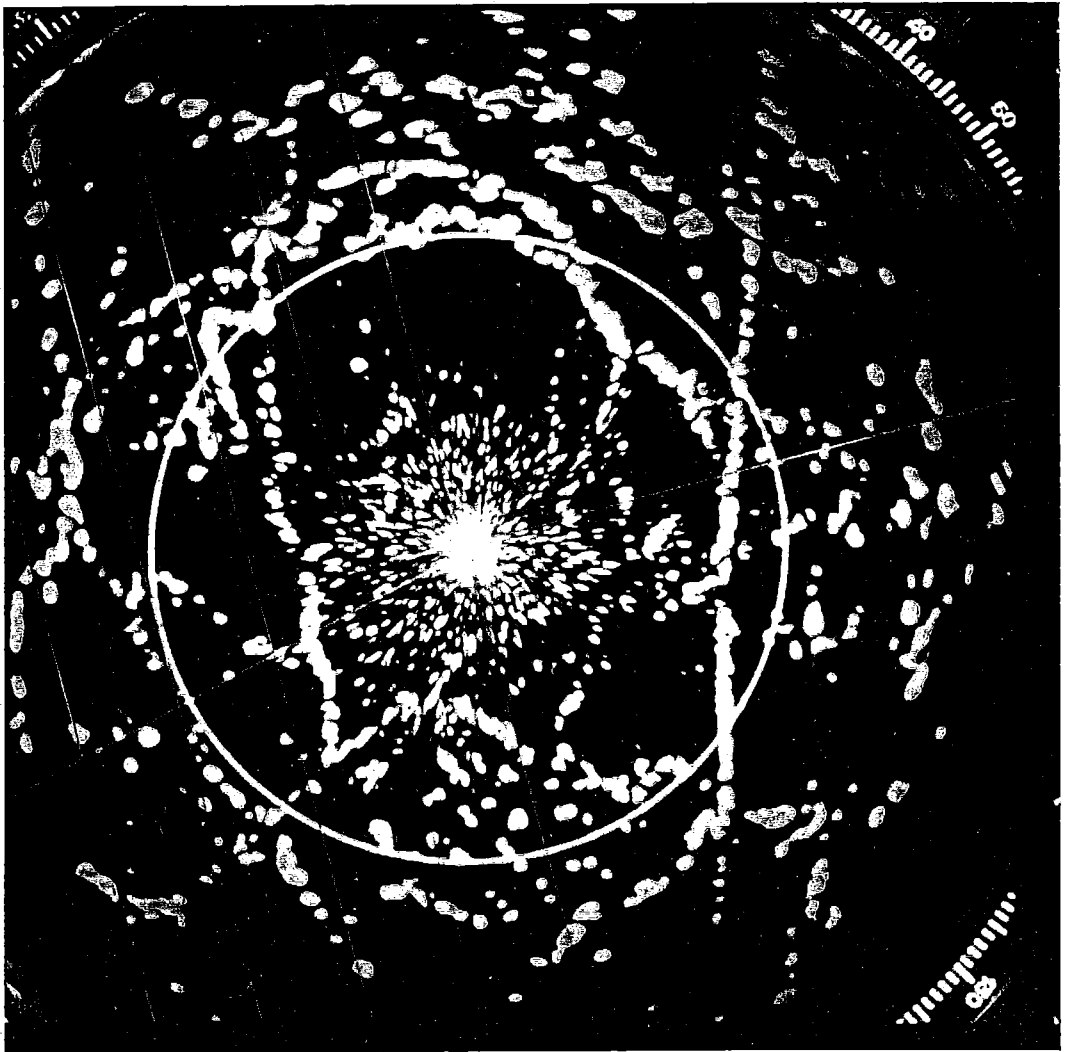


Figure 23—25. Comparison between photos S-band radar — SLAR — X-band radar.

Figure 23.

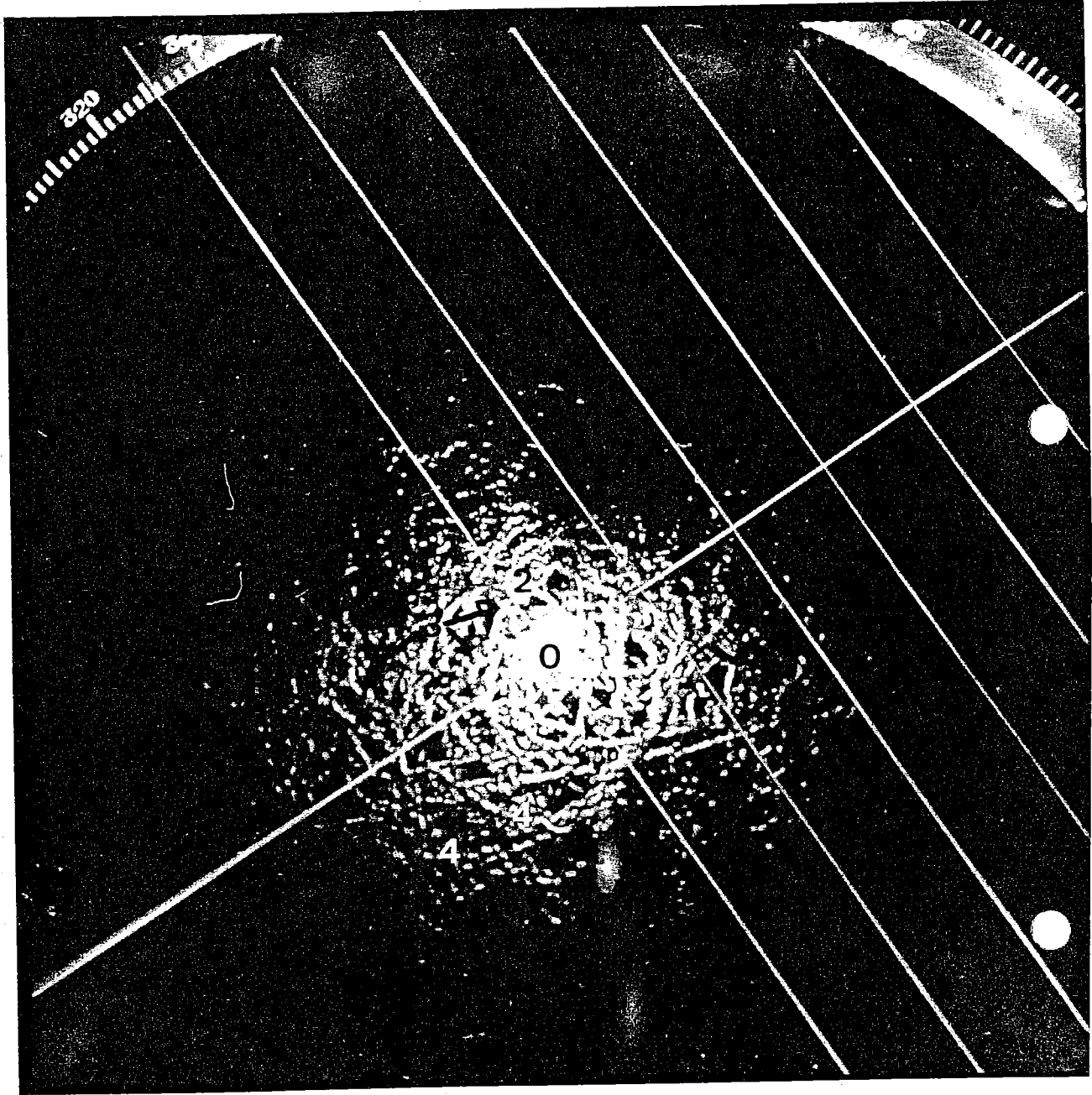


Figure 24.



Figure 25.

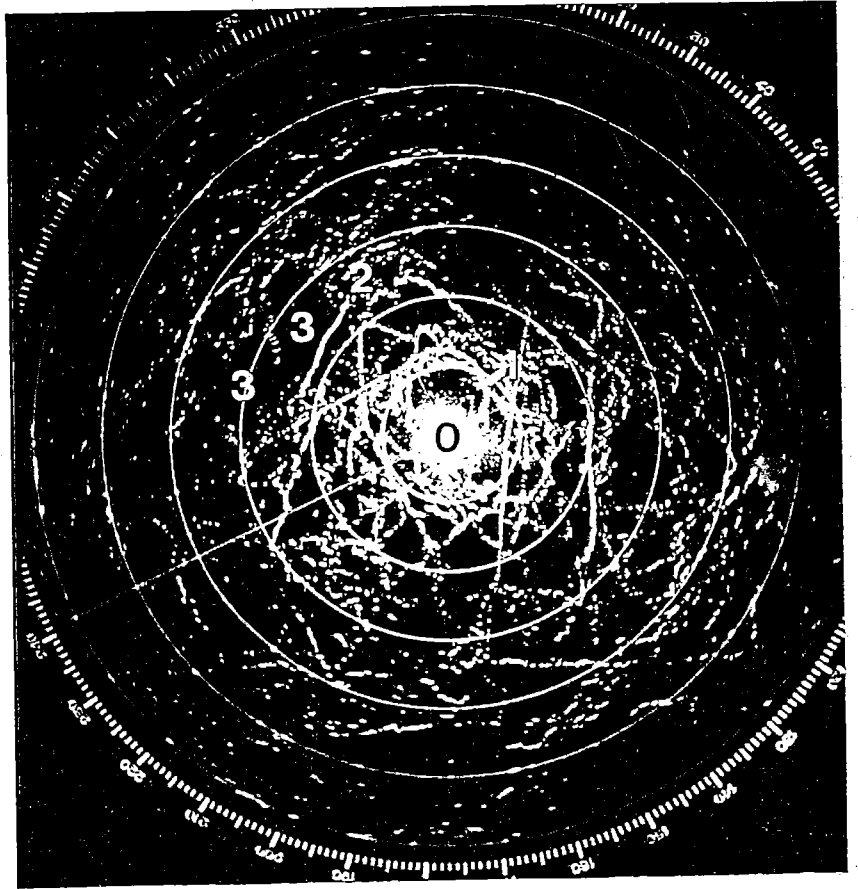
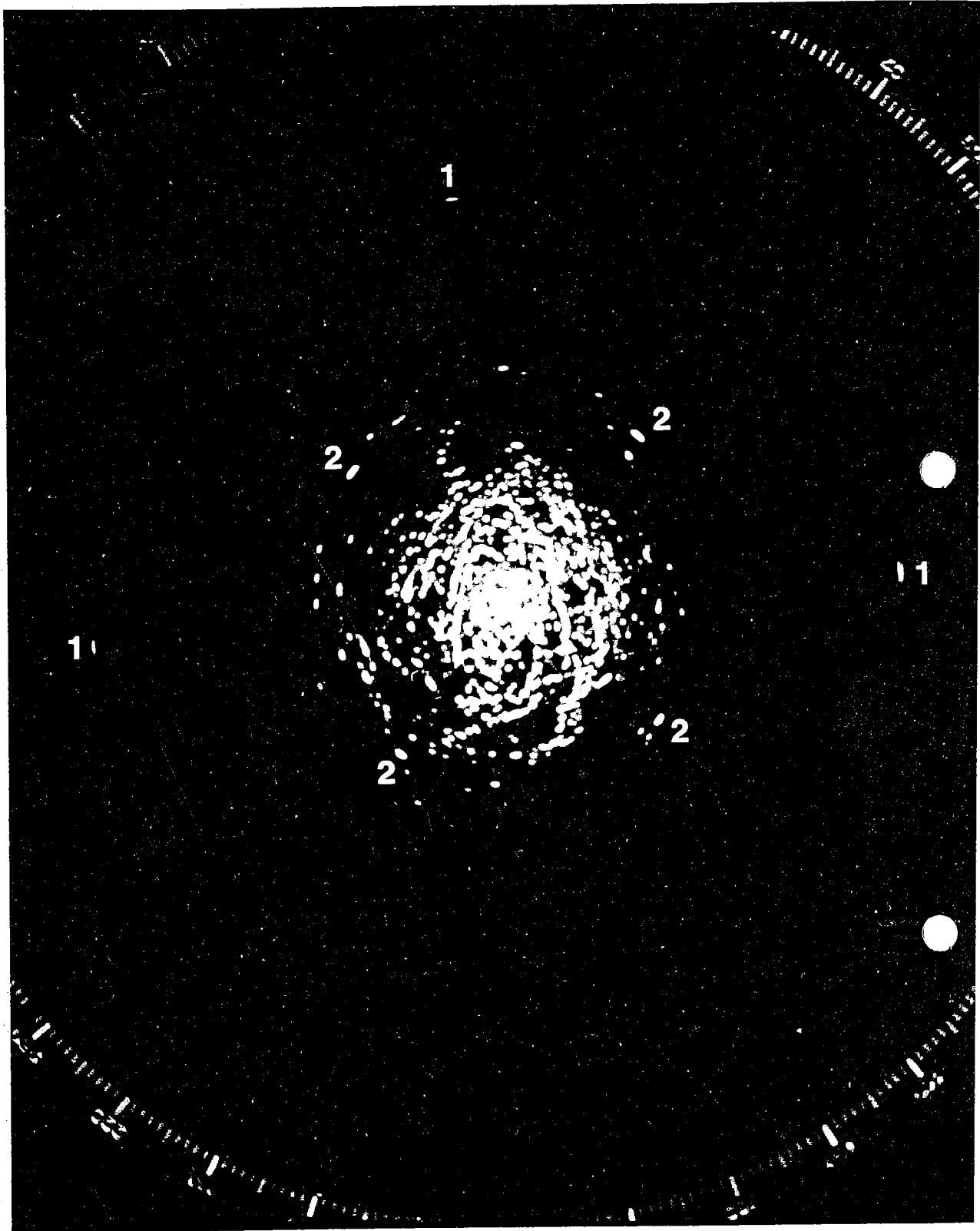


Figure 26. S-band radar photo with echoes from the radarreflectors of the 15x15 km and 5x5 km areas.



## 4. Discussion

### 4.1 Radar signatures of different types of ice

The radar echo from one element of resolution of the radar is a sum of signal components from many discrete scatterers on the ice, ice edges, cracks, ridges etc. Thus the radar echo from one part of the ice is a measure of the local ice roughness. It is to be noted that many small scatterers, as for instance packed drift ice, can give rise to larger signals than isolated ridges on relatively flat solid ice. It should however in most cases be possible to distinguish between these types of ice structures from their surroundings. Narrow openings in the ice smaller than the resolution of the radar will also give radar signatures similar to those obtained by ridges. Areas with flat ice and open water look very similar but probably cause only minor problem for a trained radar operator due to different occurrence and shape. Thus it should be possible to use a suitable designed radar system to map the ice concentration and the structure of the ice to limits determined by the resolution of the actual system.

### 4.2 Range limitations

The results of the measurements indicate that the range limit is determined mainly by the flight altitude. It seems likely that the ice can be mapped out to a distance where the angle between the line of sight from the aircraft and the main ice level is approximately  $0.5^\circ$ . At these small grazing angles high ice ridges will cause shadow sectors. A 3 m ice ridge will have a shadow sector of 300 m within which small scale ice roughness is invisible. This will, however, in many cases be obscured by the resolution of the radar indicator and by the operator as  $0.5^\circ$  and flight altitude 2000' means a radius of the mapped area of approximately 63 km and details smaller than 300 m will hardly be noticed by the operator using this scale of mapping to get an overlay map of the ice situation.

### 4.3 Mapping capacity of airborne radars

The mapping capacity of any radar system will be determined by the resolution specified by the user of the information. Simultaneous mapping at different resolutions may be accomplished by switching the radar range and pulselength during the flight as described in the flight program for the SLAR (1). System resolution will be limited by one, or a combination of the following parameters, pulse length, antenna beamwidth, resolution of the display, operators ability, signal processing capacity, platform stability or ultimately propagation properties of the atmosphere. The most severe limitation of an airborne radar is the horizontal beamwidth of the antenna due to limited antenna dimensions.

In this report some examples of radar maps of different resolution have been given. High resolution maps from the icebreaker. Tor, medium resolution maps FLAR (range scale 20 km) and low resolution overlay maps from FLAR and ODAR. Table summarizes the mapping capacities of the radars at minimum and maximum usable range scales.

Radar	Range (km)	Mapping capacity (km <sup>2</sup> /hour)	Resolution at edge of swath (determined by pulse length and antenna beamwidth)
ODAR	2.6	990	50 m x 140 m
	63	23 900	120 m x 3 300 m
FLAR	20	7 000	45 m x 1 060 m
	80	27 500	150 m x 3 900 m
FLAR	20	22 400	45 m x 1 060 m
800*)	80	88 000	150 m x 3 900 m

\*) FLAR<sub>800</sub> same radar as FLAR in high speed aircraft.

#### 4.4 Weather dependence

Weather conditions will have a minor influence on the performance of an X-band radar system used for sea ice mapping. Heavy rain or snowfall (wet snow) may obscure parts of the mapped area but hardly affect the mapping range of the system. The effects of rain and snow especially at short ranges can be reduced by differentiating the video signal. This technique is a standard feature on most radars used for navigational purposes. The differentiation breaks up the precipitation clutter leaving the leading edge of the clutter cell as a bright line allowing the ice-echoes, which are highly variable as a function of distance, to be mapped.

Other meteorological conditions clouds, fog etc as well as light conditions will not affect the radar.

## 5. Conclusions and Recommendations

The experiences gained during Sea Ice 75 clearly support the use of airborne radar to map the ice. Simple and inexpensive conventional radars can map the large scale ice structure of extensive areas in short time in sufficient detail to assist navigation and iceforecasting. If sufficient time is available mapping of small areas with a resolution comparable to that obtained from the radars of an icebreaker is possible.

A trained radar operator should be able to extract information on type of ice, location of bigger leads and areas of heavily ridged ice. New ice and open water without sea scatter can not be distinguished from each other. The thin new ice will however be of little importance to shipping. Old level ice along the coasts will also have a similar appearance as open water, but should in most cases be separated from open water by a line of cracked or ridged ice with high reflectivity. Large scale ice drift will be found from repeated low resolution mapping.

The real time presentation and the possibility of mapping at different scales is of great importance to the radar operator as it gives an opportunity to get a quick look at the gross ice situation and direct the high resolution mapping to important areas.

Before operational systems for radar mapping of sea ice are defined further measurements of radar signatures of different types of ice are required. The preliminary measurements performed during Sea Ice 75 give examples of relative levels of reflectivity but needs a complement of backscatter measurements with calibrated radars (scattrometers) and simultaneous measurements of relevant iceparameters. These radar measurements could be performed either from landbased or shipborn stations.

Recording of radar information may be done in several ways. Photographic recording as described in this report has the drawbacks of poor dynamic range and relatively long processing time.

Radar video and antenna bearing information may also be recorded on video tape. This method preserves the full dynamic range of the radar signal and allows the analyzer to choose range scales and signal processing techniques adapted to known characteristics of radar backscatter from sea ice. A special indicator equipment is however required on board the icebreaker to replay the radar information.

At present portable TV-cameras and video recorders are used for ice reconnaissance from helicopters. Using suitable adapters for the camera it should be possible to record the PPI of a radar on board the helicopter and replay it on a standard TV-monitor. The resolution of the TV-equipment is comparable to the operational resolution of a small standard PPI. The scan conversion from the radial scan of the radar to the horizontal line scan of the vidicon causes some loss of information as only the afterglow of the radar indicator will be recorded. The method is however straightforward and should be tested as it requires no special display equipment.

## References

1. Remote Sensing of Sea Ice in the Gulf of Bothnia, March 1975, Programme, A Blomquist, C Pilo and T Thompson.
2. Ice Detection by SLAR, Results of a field experiment in the Gulf of Bothnia in March 1975, R H J Morra, Rijkswaterstaat, Netherlands, G P deLoore, Physics Laboratories TNO, Netherlands.

SWEDISH/FINNISH WINTER NAVIGATION  
RESEARCH BOARD  
REPORTS

- | No.  | Titel  |
|------|--|
| 1.   | HAVSISKONFERENS. Protokoll (1972).   |
| 2.   | VINTERSJÖFART I BOTTENHAVET — Erfarenheter av SCA:s distributionssystem — L. Sjöstedt och S. Hammarsten (1972).  |
| 3.   | ISSKADOR PÅ FARTYG I ÖSTERSJÖN, BOTTENHAVET OCH BOTTENVIKEN. — Statistisk analys av skadefrekvenser — L. Sjöstedt och S. Hammarsten (1973).  |
| 4.   | PROPELLERPROBLEM. Propellerverkningsgradens beroende av bladutformningen. H.P. Loid (1973).  |
| 5.   | FARTYGS FRAMDRIVNINGSMOTSTÅND I IS. E. Enkvist (1974).   |
| 6.   | VINTERSJÖFART MED STORA FARTYG I BOTTENVIKEN. (1974).  |
| 7.   | VINTERSJÖFART I BOTTENVIKEN. Symposium Luleå (1974).   |
| 8.   | HAVSISUNDERSÖKNINGEN I BOTTENVIKEN VINTERN 1974. A. Omstedt, T. Thompson och I. Udin (1974).   |
| 9.   | KARTERING AV YTVATTENTEMPERATUREN I VATTNEN RUNT SVERIGE. J-E. Lundqvist, A. Omstedt och I. Udin (1974).   |
| 10.  | EXPERIMENTS ON REMOTE SENSING OF SEA ICE USING A MICROWAVE RADIOMETER. M. Tiuri, M. Hallikainen and K. Kaski (1974).   |
| 11.  | BOTTENVIKENS STÅLFYRAR — HÅLLFASTHETSANALYS OCH FÖRBÄTTRINGSFÖRSLAG. M. Määttänen (1974).  |
| 12.  | FORMATION AND STRUCTURE OF ICE RIDGES IN THE BALTIC. E. Palosuo (1975).  |
| 13.  | CALCULATION OF ICE DRIFT IN THE BOTHNIAN BAY AND THE QUARK. A. Valli and M. Leppäranta (1975).   |
| 14.  | A NARROW BEAM SONAR TO MEASURE THE SUBMARINE PROFILE OF AN ICE RIDGE. E. Palosuo, T. Pousi and M. Luukkala (1976).   |
| 15.  | THE AVERAGE SURFACE TEMPERATURE IN THE AUTUMN AND THE EARLY WINTER ON THE GULF OF BOTHNIA, THE NORTHERN BALTIC SEA AND THE GULF OF FINLAND (1966—1974). H. Grönvall and E. Palosuo (1976). |
| 16:1 | SEA ICE -75. Programme. Å. Blomquist, C. Pilo and T. Thompson (1975).  |
| 16:2 | SEA ICE -75. Ground truth report. I. Udin (1976).  |
| 16:3 | SEA ICE -75. Ice detection by SLAR. R.H.J. Morra and G.P. de Loor (1976).  |
| 16:4 | SEA ICE -75. Analysis of SLAR data. S. Parashar (1976).  |
| 16:5 | SEA ICE -75. FLAR, ODAR, ship's radar. J. Nilsson, T. Hagman and Y. Nilsson (1976).  |
| 16:6 | SEA ICE -75. IR-scanner results. E. Fagerlund and G. Lundholm (1976).  |
| 16:7 | SEA ICE -75. Radaraltimeter results. S. Axelsson (1976).   |
| 16:8 | SEA ICE -75. Dynamical report. I. Udin and A. Omstedt (1976).  |
| 16:9 | SEA ICE -75. Summary report. Å. Blomquist, C. Pilo and T. Thompson (1976).   |

